Cytological Diagnosis Based on Fuzzy Neural Networks

Konstantinos Blekas, Andreas Stafylopatis
National Technical University of Athens
Department of Electrical and Computer Engineering
157 73 Zographou, Athens, Greece
E-mail: kblekas/andreas@cs.ntua.gr

Dimos Kontoravdis
01-Pliroforiki S.A., 111 43 Athens, Greece
E-mail: dkont@01p.gr

Aristidis Likas
University of Ioannina
Department of Computer Science
451 10 Ioannina, Greece
E-mail: arly@cs.uoi.gr

Petros Karakitsos
Department of Clinical Cytology and Cytogenetics
Laiko Hospital, Athens, Greece

Abstract

A diagnostic system is presented that employs morphometry combined with a fuzzy neural network approach, for the discrimination of benign from malignant gastric lesions. The input to the system consists of images of routine processed gastric smears stained by Papanicolaou technique. The analysis of the images provides a data set of cell features. The fuzzy min-

max neural network classifier, an efficient pattern recognition approach, is used to classify benign and malignant cells based on the extracted morphometric and textural features. The fuzzy min-max classification network is based on hyperbox fuzzy sets and can be incrementally trained requiring only one pass through the training set. The application of the fuzzy min-max neural network yields high rates of correct classification at both the cell level and the patient level. These results indicate that the use of intelligent computational techniques along with image morphometry may offer very useful information about the potential of malignancy of gastric cells.

Key Words

Cytological diagnosis, fuzzy min-max neural network, image morphometry, classification.

1. Introduction

The diagnostic process used in Image Cytometry aims to exploit information extracted from medical images. In usual real life situations, cytopathologists look through the microscope and make a diagnosis probably using a subconscious process based on pattern recognition. Therefore, in practice it is quite difficult to extract and formulate the expert knowledge used by a cytopathologist during diagnosis. The problem in diagnosis is to map the morphometric quantitative descriptions measured to the known qualitative pathological entities.

The application of intelligent computational techniques, such as neural networks and fuzzy systems, seems to provide a solution to the above situation and constitutes a new emerging field in Diagnostic Cytology. Pattern recognition, data base search, knowledge extraction and decision-making, are some of the most important applications of neural networks in

the field of Cytology (Dawson, 1991; Astion and Wilding, 1992a; Astion and Wilding, 1992b; Truong, 1995). Up to now neural networks have been successfully applied for the mass screening of Gynaecological Cytology samples (Rosenthal and Mango, 1994).

Gastric Cytology has not reached wide acceptance in the investigation of gastric lesions because of the difficulties in the discrimination of benign lesions with severe regenerative alterations from well differentiated cancer cells (Kasugai and Kobayashi, 1974; Husain, 1991). However the same diagnostic dilemmas are also present in tissue sections from gastric mucosa biopsies with dysplastic or regenerative changes.

The diagnostic system described in the present paper exploits the potential of morphometry combined with fuzzy neural networks in the discrimination of benign from malignant gastric cells in routine prepared gastric smears, and provides a useful medical expert tool that can be very helpful to cytopathologists.

Fuzzy min-max neural networks (Simpson, 1992; Simpson, 1993; Likas *et al.*, 1994) constitute one of the many models of computational intelligence that have been recently developed from research efforts aiming at synthesizing neural networks and fuzzy logic (Bezdek, 1992; Kosko, 1992; Kartalopoulos, 1996).

The fuzzy min-max classification neural network (Simpson, 1992) is an on-line supervised learning classifier based on *hyperbox* fuzzy sets, which are regions of the pattern space that can be completely defined by the minimum and the maximum points along each dimension. In the case where a pattern is not completely contained in any of the hyperboxes, a properly computed fuzzy membership function indicates the degree to which the pattern falls outside of each of the hyperboxes. Learning in the fuzzy min-max classification network is an *expansion-contraction* process that consists of creating and adjusting hyperboxes and also associating a class label to each of them. During operation, the class associated with the hyperbox having maximum membership is taken as the decision of the network. An extension of the original definition and operation of the model has been

developed (Likas *et al.*, 1994) in order to apply the method to pattern recognition problems that involve both discrete and continuous attributes.

In the following section the application setup and study design are described. In Section 3 a brief description of the operation and training of the fuzzy min-max classification network is provided. Section 4 represents results from the application of the fuzzy min-max method to the classification of gastric cells. Evaluation of the proposed approach and discussion are provided in Section 5.

2. System Description and Study Design

2.1. System Components

The diagnostic process is complex and can be split into several stages. Figure 1 displays a general schema of the process characterizing the operation of the diagnostic system. It is actually composed of four stages, namely: Image Acquisition, Image Processing, Feature Selection and Classification.

The first stage involves the capturing and analysis of the microscopic images and is very difficult because of the presence of noise and the complexity of the image. The elimination of noise is essential for the cell image acquisition module. The source of the noise is either the sample itself and/or the miss-calibrated microscope parameters. The process applied for the elimination of noise is median filtering which reduces the image random noise, while keeping all the initial information.

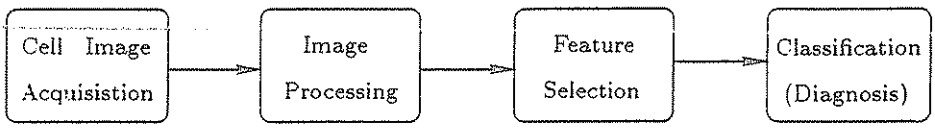

Fig. 1: System description

During median filtering the image array is scanned using 3x3 templates (line by line and column by column). For each template, the grey values included in this 3x3 template are sorted and the central pixel of the template is replaced by the median value of the sorted list. Noisy values (if present in the template) are placed at the edges of the sorted list. The median value of the list, that replaces the central pixel of the template, is most probably a true value (not noise) which was initially contained in the image.

The noise that comes from the microscope parameters (i.e. noise on the microscope optical parts) can only be reduced by carefully clearing the corresponding parts using special liquids.

The correct calibration of the microscope is another essential step for successful classification of the cells. The method used is based on the digitization of a standard sample through the microscope. This sample does not contain any cells in the field of view (empty field). The system analyses this sample and extracts various parameters that characterize the noise percentage of the microscope system, lighting and focusing conditions etc. The extracted parameters are compared with the predefined calibration ones resulting to a measure that identifies the capturing behaviour of the system.

Segmentation of cytoplasm and the cell nuclei is performed during the second stage. To achieve this, a suitable preprocessing of the image is applied in such a way that a global threshold based on the histogram can segment the cell nuclei and the cytoplasm. The preprocessing involves image filtering and enhancement of the cell nuclei. Enhancement of the cell nuclei increases the contrast between the nuclei and the background. This enhancement is carried out using min filtering.

The characteristics for the discrimination of cells involve two general categories: geometric characteristics and characteristics that are based on individual pixel values (optical or density features). The following sub-section provides a more detailed description of the above characteristics.

2.2 Specimens and Extracted Features

Sixty eight patients with gastric lesions were investigated in studying the proposed diagnostic approach. The study was performed on brushing

cytology smears taken during endoscopy. The smears were routinely fixed in 96° ethanol for 30 minutes and stained with Papanicolaou technique. The cytological diagnosis was made by at least two cytopathologists with 10 years experience in gastric cytology and was also confirmed by the histologic examination of biopsies and/or surgical specimens. The output of the cytological examination assigns a cell to one of five classes (cancer, gastritis, inflammatory dysplasia, true dysplasia and ulcer). The correlation of the cytological with the final diagnosis (referring to three classes, namely cancer, gastritis and ulcer) is presented in Table 1.

Table 1

Correlation of final and cytological diagnosis

	Final diagnosis		
Cytological diagnosis	cancer	gastritis	ulcer
cancer	19		
gastritis		18	
inflammatory dysplasia			3
true dysplasia	4		
ulcer			24

The basic measurements/features that are extracted from every cell can be grouped according to their physical characteristics into two main categories: *geometric* and *densitometric*}.

The geometric features are extracted both from the nucleus and the cytoplasm, according to the computational method and the mathematical models reported in the literature (Baak, 1991; Baxes, 1994; Sonka *et al.*, 1994). These characteristics describe properties relative to the size (e.g. area, perimeter, diameter etc.) or properties that give information about the shape (e.g. Form area, Form perimeter etc.) as well as the relative position of the nuclei inside the cell. When the cytoplasm is absent the geometric features of the

nucleus. The feature `mean radius' of the nucleus is considered as the mean value of the mean radius of all the nuclei included in the cell; for a cell with one nucleus or for a naked nucleus it is considered equal to the mean radius of the nucleus.

Other features that are also extracted are: a) the number of nuclei per cell; if it is a naked nucleus this feature is taken equal to one, b) the mean value of the length of the axes that connect the cell center of mass and the nuclei centers of mass; if it is a naked nucleus this feature has a value of zero (as if one nucleus is in the center of the cell), and finally c) the nucleo-cytoplasmic ratio, which is considered equal to one if the cytoplasm is absent.

The densitometric features provide textural information about nuclei. From the various methods that have been proposed for the description of chromatine texture, it was preferred to implement four models: Histogram, Differences Histogram, Run Length and Co-occurrence Matrix. The first two models have the advantage of computational simplicity at the cost of poor texture discrimination, while the last two models give more precise information on the nuclei structure. The histogram of an object represents the relative frequency of occurrence of the various gray levels in the image, while the differences histogram method provides features by computing the difference of each pixel value from the neighbouring pixels that lie at a specific distance. The run length method reveals directional and coarseness information about the texture. Finally, the co-occurrence matrix gives the joint probability of two pixels lying at a specific distance in the image.

During this study never was a cell encountered with more than one nucleus, so each cell was represented by a vector with 41 elements: 12 geometric features for the nucleus, 12 geometric features for the cytoplasm, the number of nuclei, the mean value of the length of the axes that connect the cell center of mass and the nuclei centers of mass, the nucleus cytoplasmic ratio, and 14 densitometric features for the nucleus. These features are displayed in Table 2, while their descriptive statistics are summarized in Appendix A.

Table 2

Features of data

Type	*Feature*
Geometric for cytoplasm	Areas of Cells
	Circularities of Cells
	Major Axis of Cells
	Minor Axis of Cells
	Perimeter of Cells
	Form area of Cells
	Form perimeter of Cells
	CI of Cells
	Contour Ratio of Cells
	Roundness Factor of Cells
	Diameter of Cells
	Mean Radius of Cells
Geometric for nucleus	Areas of Nuclei
	Circularities of Nuclei
	Major Axis of Nuclei
	Minor Axis of Nuclei
	Perimeter of Nuclei
	Form of Nuclei
	Form perimeter of Nuclei
	CI of Nuclei
	Contour Ratio of Nuclei
	Roundness Factor of Histogram
	Diameter of Nuclei
	Mean Radius of Nuclei in Cell
Densitometric (textural information about nuclei)	Mean of Nuclei Histogram
	Std of Nuclei Histogram
	Var of Nuclei Histogram
	Run Length Short Run of Nuclei
	Run Length Long Run of Nuclei
	Run Length Gray Level of Nuclei
	Run Length Distribution of Nuclei
	Cooccurrence Matrix Maximum of Nuclei
	Cooccurrence Matrix Entropy of Nuclei
	Cooccurrence Matrix Inertia of Nuclei
	Mean of Differences Histogram
	Variance of Differences Histogram
	Contrast of Differences Histogram
	Entropy of Differences Histogram
Other	Nuclei Cytoplasm Ratio
	Nuclei per Cell
	Mean Distance of Nuclei in Cell

3. The Fuzzy Min-Max Classification Network

We have selected a fast and efficient mechanism for the classification part of the diagnostic system, the fuzzy min-max neural network classifier.

The fuzzy min-max neural network is an on-line supervised learning classifier whose operation and training are based on the concepts of hyperbox fuzzy sets. Consider a classification problem with n continuous attributes that have been rescaled in the interval [0,1], hence the pattern space is I^n ([0, 1]^n). Moreover, consider that there exist p classes and B hyperboxes with corresponding minimum and maximum values v_{ji} and w_{ji}, respectively (j=1,...,B, i=1, ...,n) (Figure 2). Let also c_k denote the class label associated with hyperbox B_k.

When the h^{th} input pattern $A_h = (a_{h1}, ..., a_{hn})$ is presented to the network, the corresponding membership function for hyperbox B_j is (Simpson, 1992)

$$b_j(A_h) = \frac{1}{n}\sum_{i=1}^{n}[1 - f(a_{hi} - w_{ji}, \gamma) - f(v_{ji} - a_{hi}, \gamma)] \qquad (1)$$

where $f(x, \gamma) = x\gamma$, if $0 \le x\gamma \le 1$, $f(x, \gamma) = 1$ if $x\gamma > 1$ and $f(x, \gamma) = 0$ if $x\gamma < 0$. If the input pattern A_h falls inside the hyperbox B_j then $b_j(A_h) = 1$, otherwise

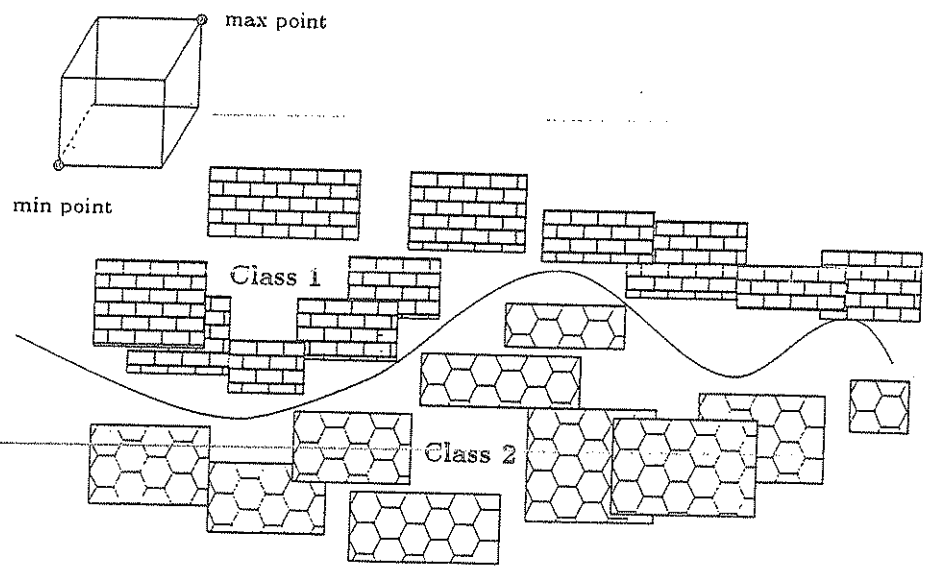

Fig. 2: Fuzzy hyperboxes

the membership decreases and the parameter $\gamma \geq 1$ regulates the decrease rate. As already noted, the class of the hyperbox with the maximum membership is considered as the output of the network.

In a neural network formulation, each hyperbox B_j can be considered as a hidden unit of a feedforward neural network that receives the input pattern and computes the corresponding membership value. The values v_{ji} and w_{ji} can be considered as the weights from the input to the hidden layer. The output layer contains as many output nodes as the number of classes. The weights u_{jk} ($j = 1, \ldots, B$, $k = 1, \ldots, p$) from the hidden to the output layer express the class corresponding to each hyperbox: $u_{jk} = 1$ if B_j is a hyperbox for class c_k, otherwise it is zero. Figure 3 represents the architecture of the fuzzy min-max classification neural network.

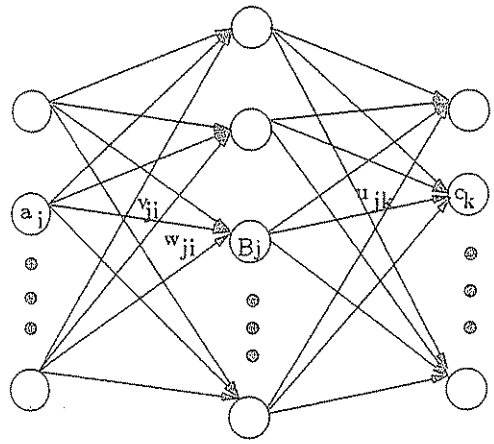

Fig. 3: Neural network formulation of the fuzzy min-max classifier

During learning, each training pattern A_h is presented once to the network and the following process takes place. First we find the hyperbox b_j with the maximum membership value among those that correspond to the same class as pattern A_h and meet the expansion criterion:

$$n\theta \geq \sum_{i=1}^{n} (\max(w_{ji}, a_{hi}) - \min(v_{ji}, a_{hi})) \qquad (2)$$

The parameter θ ($0 \leq \theta \leq 1$) is a user-defined value that imposes a bound on the size of a hyperbox and its value significantly affects the effectiveness of the training algorithm. In the case where an expandable hyperbox (of the same class) cannot be found, then a new hyperbox B_k is spawned and we set $w_{ki} = v_{ki} = a_{hi}$ for each i. Otherwise, the hyperbox B_j with the maximum membership value is *expanded* in order to incorporate the new pattern A_h, i.e., for each $i = 1, \ldots, n$:

$$v_{ji}^{new} = \min(v_{ji}^{old}, a_{hi}) \tag{3}$$

$$w_{ji}^{new} = \max(w_{ji}^{old}, a_{hi}) \tag{4}$$

Following the expansion of a hyperbox, an *overlap test* takes place to determine if any overlap exists between hyperboxes from different classes. In case such an overlap exists, it is eliminated by a *contraction* process} during which the size of each of the overlapping hyperboxes is minimally adjusted. Details concerning the overlap test and the contraction process can be found in (Simpson, 1992). The effectiveness of the training algorithm generally depends on two factors: the value of the parameter θ and the order with which the training patterns are presented to the network.

4. Results

The image analysis part of the system is composed of an IBM compatible Pentium 133MHz computer, equipped with a 1MB Matrox MVP-AT frame grabber and a SONY DXC-151P color CCD camera. The camera is attached to a Nicon Labophot 2 microscope through a C-mount adapter and to the frame grabber by proper cabling. The CCD sensor of the camera has a resolution of 756x581. All images were captured using a 40x objective and digitized to 512x512 pixels.

The imaging software operates under MS-Windows and is used for the segmentation of cells and their nuclei and for the extraction of the

measurements that correspond to the features. The S/W is in a high degree customized. A commercially available image processing product is used (OPTIMAS from BioScan Inc.) which supplies a variety of image processing functions and the ability to extract basic geometric and densitometric characteristics from images or parts of images. On the top of this package is applied a library of custom functions. These are written in C (mainly for the segmentation and for texture estimation) and in the macro language that OPTIMAS supports (ALI=Analytical Language for Images) for the user interface, for image storage/retrieval, storage of measurements and for the extraction of texture features.*

The study group of our system consisted of data from 68 patients with gastric lesions. Using the custom image analysis described above, these cases provided a data set of 5933 cells (see Table 3). Before entering the data set into the fuzzy neural network classifier the feature values were normalized to the interval [0, 1], as prescribed by the classifier model.

In order to evaluate the overall performance of our system four different series of experiments were carried out with respect to the level of examination and the number of classes.

With respect to the level of examination experiments were conducted considering both individual cells randomly selected from the total cell

Table 3

Data set

	5 classes					2 classes	
	Cancer	Gastritis	I-dyspl	T-dyspl	Ulcer	Malignant	Benign
Cells	851	2078	148	171	2685	1022	4911
Patients	19	18	3	4	24	23	45

I-dyspl : Inflammatory dysplasia
T-dyspl : True dysplasia
Malignant : Cancer and T-dyspl
Benign : Gastritis, I-dyspl and Ulcer

*The development of the imaging system has been financially supported in part by 01-Pliroforiki SA under EC Project VALUE/CCS.

collection (*cellular*} level) and the total number of cells belonging to a specific patient (*patient*} level), in order to characterize a patient case. At the patient level the input pattern presented to the system consisted of the mean and standard deviation of the values of the 41 features regarding the cells obtained from that patient. At the cellular level 1785 cases were used as the training set for the fuzzy min-max neural network classifier, while the remaining 4148 cells were used as the testing set. At the patient level 23 patient cases were used as training set and the other 45 as testing set.

From another point of view, we can divide the above two datasets into either five or two classes. In other words we may represent the problem either as the discrimination of five classes (cancer, gastritis, inflammatory dysplasia, true dysplasia, and ulcer) or as a more coarse classification problem involving only two classes: malignant and benign, that can be obtained from the union of the cancer and true dysplasia cases to one class (malignant), and the three other cases to another class (benign).

From the above analysis it is clear that we can examine the performance of our system in four different classification problems. Table 4 shows the training set for the four cases that was randomly composed by selecting 30\% of the entire dataset, while Table 5 represents the respective testing set for the same classification problems.

Table 4

Training set

	5 classes					2 classes	
	Cancer	Gastritis	I-dyspl	T-dyspl	Ulcer	Malignant	Benign
Cells	257	626	44	50	808	307	1478
Patients	6	6	2	2	7	8	15

Table 5

Testing set

	5 classes					2 classes	
	Cancer	Gastritis	I-dyspl	T-dyspl	Ulcer	Malignant	Benign
Cells	594	1452	104	121	1877	715	3433
Patients	13	12	1	2	17	15	30

The performance of the fuzzy min-max neural network classifier was evaluated for all four classification problems. The diagrams in Figures 4 and 5 concern the problems of five classes and two classes respectively and draw up the correct classification rate at the cellular level. Different values of the parameter θ are considered in the range of [0.09, 0.20] with a 0.01 step. For all the obtained rates the number of constructed hyperboxes (B) is also represented. As shown by the diagrams, in the case of five classes the best classification rate was 95.18% and was obtained for the value θ = 0.1, where the neural network contained 537 hyperboxes. Table 6 illustrates the success rate at the cellular level obtained by the best fuzzy min-max neural network constructed, by providing the classification rate for each of the five classes together with the distribution of misclassified cases. For example, the correct classification rate in the case of cancer is 90.74% and erroneous

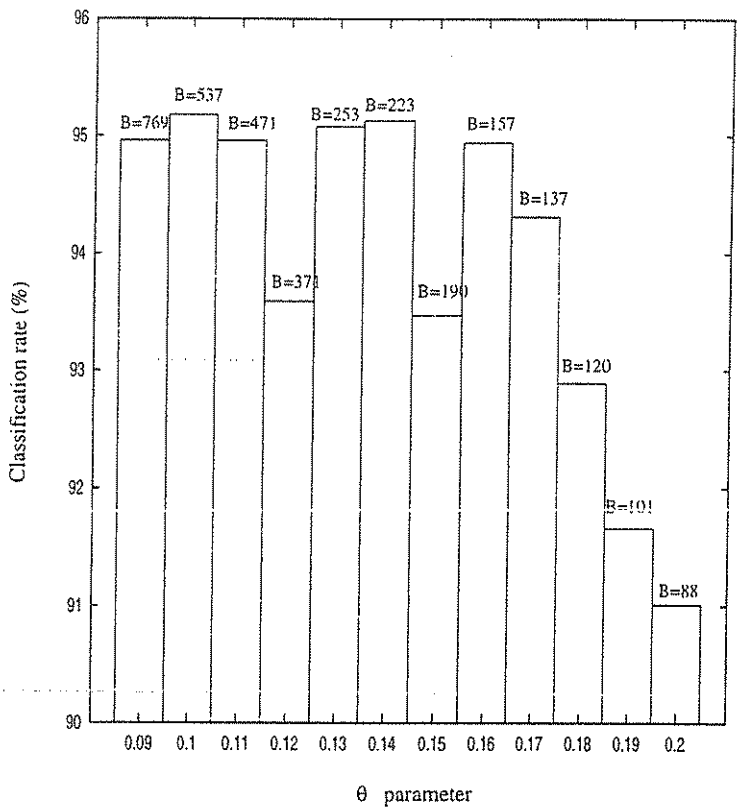

Fig. 4: Classification performance for 5 classes

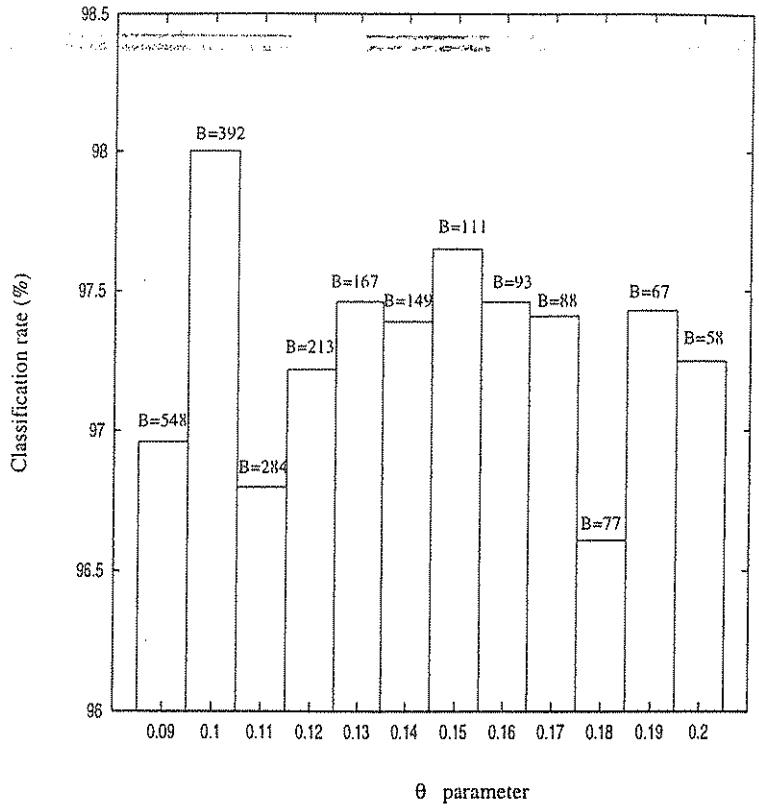

Fig. 5: Classification performance for 2 classes

Table 6

Percentages of success and failure (cellular level) of fuzzy min-max

		Fuzzy Min-Max Classification Network				
		Distribution of failure				
	Success	Cancer	Gastritis	I-dyspl	T-dyspl	Ulcer
Cancer	90.74%		65.5%	6.9%	5.2%	22.4%
Gastritis	96.90%	17.8%		11.1%	2.2%	68.9%
I-dyspl	91.35%	11.1%	33.3%		11.1%	44.5%
T-dyspl	56.20%	30.2%	7.5%	20.8%		41.5%
Ulcer	98.14%	20.0%	40.0%	25.7%	14.3%	

classification cases are assigned to gastritis at 65.5%, inflammatory dysplasia at 6.9%, true dysplasia at 5.2% and ulcer at 22.4%.

Experiments of the two-class problem considering different θ values gave a best classification rate of 98.0% at the value $\theta = 0.1$ with a network of 392 hyperboxes. The neural network classified the malignant cells with a correct rate of 91.75% while the benign cells were almost perfectly classified (99.30%).

At the patient level the fuzzy neural network classifier was trained and tested in the same manner considering five classes and two classes. In the two cases the network gave a correct overall classification rate of 93.34% and 97.78% respectively, almost irrespective of the θ values taken in the range [0.09, 0.2]. The number of constructed hyperboxes was 20 in the case of five classes and 17 in the case of two classes. Considering five classes the network confused only the two dysplasia classes (inflammatory and true) matching them as ulcer class. During the testing operation with two classes (malignant and benign) the neural network responded almost perfectly, making only one erroneous diagnosis of malignant class. It must be noted that in all the above experiments the value of the parameter γ was the same (equal to 2.0).

In order to assess the potential of the fuzzy min-max algorithm, we have also applied *learning vector quantization* to the four classification cases using the same data. For that reason we have selected the LVQ1 algorithm (Kohonen, 1990). A sufficient number of 'codebook vectors' for the four classification problems (2 for the cellular level and 2 for patient level) was found to be 40, 20, 10 and 10 respectively. The learning parameter α was set initially to a small value 0.04 and was linearly decreased with time. Table 7 shows the performance of the LVQ1 algorithm in comparison with the results of the fuzzy min-max method, i.e. the classification rate of the testing set for all four cases. Moreover, Table 8 provides an analysis of the success rate obtained by the LVQ1 algorithm at the cellular level, in contrast to Table 6 which concerns the fuzzy min-max network. The superiority of the fuzzy min-max algorithm is apparent from the above tables that illustrate the capability of the method to eliminate overlapping in the feature space.

Table 7

Comparison of fuzzy min-max and LVQ

		Fuzzy Min-Max	*LVQ1*
Cells	5 classes	95.18%	87.73%
	2 classes	98.00%	92.02%
Patients	5 classes	93.34%	64.44%
	2 classes	97.78%	95.56%

Table 8

Percentages of success and failure (cellular level) of LVQ

		Learning Vector Quantization				
		Distribution of failure				
	Success	Cancer	Gastritis	I-dyspl	T-dyspl	Ulcer
Cancer	78.28%		41.1%	4.6%	21.7%	32.6%
Gastritis	91.25%	42.5%		4.7%	20.5%	32.3%
I-dyspl	92.30%	37.5%	0.0%		62.5%	0.0%
T-dyspl	76.03%	48.2%	3.5%	34.5%		13.8%
Ulcer	88.49%	27.4%	44.9%	6.9%	20.8%	

5. Discussion

Cytology has not reached a wide acceptance in the investigation of gastric lesions because of the relatively high rate of false negative and false positive results. However the same problems may also occur in histologic examination of tissue biopsies (Kasugai and Kobayashi, 1974; Husain, 1991).

The aim of this study was to investigate the potential role of a diagnostic system in the area of gastric cytology. We have tried to apply effective methods from the fields of medical analysis and pattern recognition in order to overcome the difficulties usually encountered by cytopathologists. The

diagnostic system is a combination of morphometry with fuzzy neural networks and the objective is to discriminate benign from malignant gastric cells in routine prepared gastric smears.

An important phase of the process was the selection of the data. The features used in our study were selected because they represent classical morphometric and textural characteristics, which correspond to objective estimation of cellular characteristics examined by the eye of a skilled cytopathologist during routine screening. Although the importance of each individual feature is out of the scope of this study, it was decided that several features be extracted from the system, as it is accepted that texture gives an indication of the DNA activation, and that changes in the nuclear and cellular size, shape and texture reflect alterations which may be accounted for in the behaviour of cells.

According to the results, the performance of the fuzzy min-max neural network was excellent in the discrimination of benign from malignant cells. Actually, at the cellular level, the network could discriminate either five classes or two general classes with a high success rate. From the results of Table 6 we can extract some significant information about the behaviour and the level of accuracy of our system. The fuzzy neural classifier responds successfully in the cases of ulcer, gastritis, inflammatory dysplasia and cancer. The low correct classification rate in the case of true dysplasia is very reasonable since this kind of cells corresponds to well differentiated carcinomas. When considering only two classes (benign, malignant) we obtained higher classification performance, 91.75% of malignant and almost 100% of benign cells. The last rate is very important for cytological diagnosis because it could reduce uncertainty.

At the patient level the results were analogous. Even though the number of data available for training was relatively small and the number of features was twice the number considered at the cellular level (by adding standard deviation), the system exhibited an excellent behaviour in both interpretations of classes, making only four and one mistakes respectively.

The inability of perfect (100%) classification of benign and malignant cells and lesions arises from the fact that in the feature space the borders of

the two classes are not always clear. This fact is displayed in Figure 6 showing benign cells from ulcer cases and corresponding cancer cells which are very similar.

Due to the overlap observed in the feature space the discrimination between benign and malignant cells using statistical classifiers has not been successful, although a statistically significant difference was observed (Danno, 1976; Boon *et al.*, 1981; Tosi *et al.*, 1987). The data set considered in our experiments has also been used to train a neural network classifier by means of the backpropagation algorithm (Karakitsos *et al.*, 1995). Although the neural network exhibited high success rates in the discrimination of two classes, it showed poor performance when tested in the classification of data into 5 classes. Back propagation suffers from the inability to build very efficient discriminating rules for significant cases of data overlapping. Also,

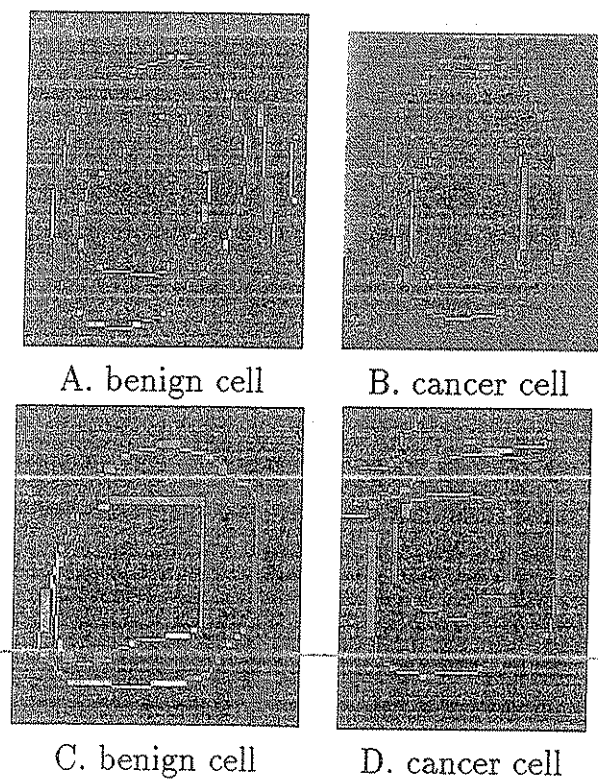

Fig. 6: Sample benign and cancer cells from ulcer cases

it has the disadvantage of requiring a large amount of time to learn the decision boundaries of the classes. On the other hand, the fuzzy min-max neural network classifier bears some desirable features which are due to the expansion, overlapping test and contraction operations. Thus, it succeeds in determining efficient building blocks (hyperboxes) and eliminating overlapping in the feature space between hyperboxes of different classes, yielding a fast learning procedure. Another important advantage of the fuzzy min-max classifier is its robustness with respect to the selection of the value of the θ parameter. As can be observed from Figures 4 and 5, the classifier shows high classification performance all over the range [0.09, 0.2] of θ.

Moreover, the effectiveness of the fuzzy min-max neural network in overcoming difficulties that arise from overlapping has been shown by means of its superiority over LVQ. It must be noted that in order to assess problem difficulty we have preferred to perform experiments with LVQ rather than consider data analysis or visualization techniques (like the one based on SOM proposed in (Mao and Jain, 1995)). The inability of methods like LVQ to achieve high recognition rates suggests that the classification problem is hard and we did not expect to obtain any significant information by performing data visualization (which is mainly based on clustering techniques).

As the experiments indicated, the fuzzy min-max classification neural network constitutes a very promising method for pattern recognition and, more specifically, for medical diagnosis applications. Indeed, through the use of fuzzy logic the system can extract useful information, such as the degree of membership of a cell data to each concerned class. Thus, a cytopathologist may obtain diagnostic opinions about whether a cell or the collection of a patient's cells belong to each category. Building efficient decision regions and fuzzy geometric structures, the fuzzy min-max neural classifier defines fuzzy internal rules providing a powerful diagnostic tool.

References

Astion, M.L. and Wilding, P, The application of back propagation neural networks to problems in pathology and laboratory medicine. *Artificial Intelligence*, 116, 995-1001 (1992a).

Astion, M.L. and Wilding, P. Application of neural networks to the interpretation of laboratory data in cancer diagnosis. *Clin. Chem.*, 38, 34-38 (1992b).

Baak, J.P.A. *Manual of Quantitative Pathology in Cancer Diagnosis and Prognosis.* Springer-Verlag, 1991.

Baxes, A.G. *Image Processing Principles and Applications,* John Wiley, 1994.

Bezdek, J. (Editor), Special Issue on Fuzzy Logic and Neural Networks, *IEEE Trans. on Neural Networks,* 3, 1992.

Boon, M.E., Kurver, P.H.J. and Baak, J.P.A. The application of morphometry in gastric cytological diagnosis. *Virchows Arch. [A],* 393, 159-164 (1981).

Danno, M. Statistical criteria for the cytology of gastric cancer, a proposal of distance index. *Acta Cytol.*, 20, 466-468 (1976).

Dawson, A.E. Nuclear grading of breast carcinoma by image analysis. *A.J.C.P.*, 95, 29-37 (1991).

Husain, O.A.N. Alimentary tract. *Comprehensive Cytology,* 409-432 (1991).

Karakitsos, P., Botsoli, S.E., Pouliakis, A., Tzivras, M., Archimandritis, A., Liossi, I.A. and Kyrkou, K. The potential of the back propagation neural network in the discrimination of benign from malignant gastric cells. *Anal. Quant. Cytol. Histol.* (1995).

Kartalopoulos, S.V. *Understanding Neural Networks and Fuzzy Logic, Basic Concepts and Applications,* IEEE Press, 1996.

Kasugai, T. and Kobayashi, S. Evaluation of biopsy and cytology in the diagnosis of gastric cancer. *Am. J. Gastroenterol.*, 62, 199-203 (1974).

Kohonen, T. The self-organization map. *Proceedings of the IEEE,* 78, 1464-1480 (1990).

Kosko, B. *Neural Networks and Fuzzy Systems, A Dynamical Systems Approach to Machine Intelligence,* Prentice-Hall, 1992.

Likas, A., Blekas, K. and Stafylopatis, A. Application of the fuzzy min-max neural network classifier to problems with continuous and discrete attributes, *Proc. NNSP'94*, Ermioni, Greece, 1994.

Mao, J. and Jain, A.K. Artificial neural networks for feature extraction and multivariate data projection. *IEEE Trans. on Neural Networks,* 6, 296-318 (1995).

Rosenthal, D.L. and Mango, L.J. Application of neural networks for interactive diagnosis of anatomic pathology specimens. *Compendium on the Computerized Cytology and Histology Laboratory,* 1004; 173-184.

Rosenthal, D.L. and Mango, L.J. Application of neural networks for interactive diagnosis of anatomic pathology specimens. C*ompendium of the Computerized Cytology and Histology Laboratory*, 1004; 173-184 (1994).

Simpson, P.K. Fuzzy min-max neural networks – part 1: Classification. *IEEE Trans. on Neural Networks,* 3, 776-786 (1992).

Simpson, P.K. Fuzzy min-max neural networks – part 2: Clustering. *IEEE Trans. on Fuzzy Systems,* 1, 32-45 (1993).

Sonka, M., Hlavac, V. and Boyle, R. *Image Processing Analysis and Machine Vision,* Chapman & Hall, 1994.

Tosi, P., Luzi, P. and Baak, J.P.A. Gastric dysplasia: A stereological and morphometrical assessment, *J. Pathol.*, 15, 83-94 (1987).

Truong, H. Neural networks as an aid in the diagnosis of lymphocyte-rich effusions. *Anal. Quant. Cytol. and Histol.*, 17, 48-54 (1995).

APPENDIX A

Table 9

Statistics of the data set

Feature	*Class*	*Mean*	*Std*	*Feature*	*Mean*	*Std*
Areas of Cells	Cancer	215.80	202.91	Circularities of Cells	14.31	19.47
	Gastritis	196.28	196.74		4.81	4.82
	I dyspl.	927.99	887.84		5.42	81.61
	T dyspl.	4.33E+3	4285.60		6.22	5.94
	Ulcer	117.282	112.29		845.39	1071.00
Major Axis of Cells	Cancer	19.11	18.76	Minor Axis of Cells	14.58	14.52
	Gastritis	4.03	4.06		2.74	2.76
	I dyspl.	9.94	9.97		7.08	10.59
	T dyspl.	18.29	15.20		8.83	6.94
	Ulcer	5.70	5.49		7.40	8.83
Perimeter of Cells	Cancer	53.52	51.05	Form area of Cells	0.05	2.11
	Gastritis	14.87	14.96		0.50	0.50
	I dyspl.	42.96	34.44		0.02	19.51
	T dyspl.	81.84	73.85		0.00	0.01
	Ulcer	9.25	7.85		24.89	33.02
Form perimeter of Cells	Cancer	0.88	0.84	CI of Cells	3.77	3.63
	Gastritis	0.38	0.38		1.86	1.86
	I dyspl.	0.31	0.03		1.31	0.33
	T dyspl.	-0.07	-0.06		1.47	1.44
	Ulcer	0.01	-0.03		0.42	0.27
Contour Ratio of Cells	Cancer	1.13	1.28	Roundness Factor of Cells	1.06	1.07
	Gastritis	1.39	1.40		1.24	1.24
	I dyspl.	0.41	1.31		0.37	0.41
	T dyspl.	0.80	0.78		0.71	0.70
	Ulcer	1.59	1.55		1.11	1.07
Diameter of Cells	Cancer	15.98	15.11	Mean Radius of Cells	7.91	8.07
	Gastritis	3.01	3.02		1.34	1.35
	I dyspl.	7.19	3.52		2.99	6.68
	T dyspl.	10.20	7.95		4.00	2.91
	Ulcer	1.84	1.33		4.65	4.76
Areas of Nuclei	Cancer	148.53	138.04	Circularities of Nuclei	14.53	15.40
	Gastritis	89.73	89.67		4.74	4.78
	I dyspl.	113.08	105.39		7.54	43.92
	T dyspl.	329.91	311.86		4.11	4.18
	Ulcer	16.02	14.79		204.77	223.10
Major Axis of Nuclei	Cancer	15.75	15.47	Minor Axis of Nuclei	12.07	11.72
	Gastritis	3.09	3.09		2.23	2.21
	I dyspl.	4.79	6.78		3.23	6.12
	T dyspl.	7.04	5.79		5.47	4.53
	Ulcer	4.53	4.23		3.96	3.92
Perimeter of Nuclei	Cancer	44.84	42.16	Form area of Nuclei	0.06	1.16
	Gastritis	11.21	11.18		0.46	0.46
	I dyspl.	19.40	16.32		0.02	13.36
	T dyspl.	31.28	27.90		0.02	0.02
	Ulcer	5.12	4.34		13.23	14.37

Table 9 (continued)
Statistics of the data set

Form perimeter of Nuclei	Cancer	0.87	0.83	CI of Nuclei	3.80	3.64
	Gastritis	0.39	0.38		1.83	1.84
	I dyspl.	0.32	0.05		1.39	0.42
	T dyspl.	-0.12	-0.12		1.37	1.38
	Ulcer	0.01	-0.02		0.43	0.27
Contour Ratio of Nuclei	Cancer	1.15	1.28	Roundness Factor of Histogram	1.07	1.07
	Gastritis	1.37	1.37		1.21	1.21
	I dyspl.	0.47	1.30		0.39	0.39
	T dyspl.	0.74	0.75		0.70	0.70
	Ulcer	1.57	1.52		1.09	1.05
Diameter of Nuclei	Cancer	13.28	12.49	Mean of Nuclei Histogram	144.39	135.67
	Gastritis	2.36	2.35		238.94	233.56
	I dyspl.	3.63	1.94		424.44	411.35
	T dyspl.	5.70	4.65		519.36	497.73
	Ulcer	1.39	1.14		55.92	53.87
Std of Nuclei Histogram	Cancer	13.14	15.57	Var of Nuclei Histogram	217.20	208.76
	Gastritis	17.82	17.84		2.5E+4	2.5E+4
	I dyspl.	14.05	59.46		7.5E+3	7.4E+3
	T dyspl.	20.04	19.57		1.4E+4	1.4E+4
	Ulcer	183.45	219.80		950.23	943.36
Run Length Sort Run of Nuclei	Cancer	1.9E+4	1.7E+4	Run Length Long Run of Nuclei	0.01	295.43
	Gastritis	8.3E+5	8.3E+5		3.51	3.51
	I dyspl.	1.4E+8	1.3E+7		0.01	8.8E+3
	T dyspl.	2.9E+7	2.9E+7		0.7	0.67
	Ulcer	1.7E+6	1.6E+6		5.5E+6	6.6E+6
Run Length Gray Level of Nuclei	Cancer	3.3E+6	3.0E+6	Run Length Distribution of Nuclei	8.4E+4	8.3E+4
	Gastritis	1.2E+10	1.2E+10		1.4E+7	1.4E+7
	I dyspl.	7.3E+9	7.3E+9		3.4E+6	4.0E+6
	T dyspl.	9.7E+11	9.7E+11		1.9E+9	1.9E+9
	Ulcer	9.2E+8	9.2E+8		1.8E+11	1.9E+11
Cooccurrence Matrix Maximum of Nuclei	Cancer	0.00	208.27	Cooccurrence Matrix Entropy of Nuclei	0.001	0.001
	Gastritis	1.66	1.66		1.54	1.54
	I dyspl.	0.00	1.78E+4		0.01	0.01
	T dyspl.	0.61	0.61		0.56	0.56
	Ulcer	3.3E+8	3.3E+8		1.35	1.35
Cooccurrence Matrix Inertia of Nuclei	Cancer	1.82	1.79	Mean of Differences Histogram	18.98	18.28
	Gastritis	6.86	6.92		59.11	59.27
	I dyspl.	17.31	16.41		28.53	23.02
	T dyspl.	33.38	32.51		36.81	37.16
	Ulcer	3.65	3.54		13.48	12.82
Variance of Differences Histogram	Cancer	333.22	325.33	Contrast of Differences Histogram	819.25	805.65
	Gastritis	5.2E+4	5.2E+4		6.8E+5	6.8E+5
	I dyspl.	5.2E+3	5.1E+3		6.3E+4	6.3E+4
	T dyspl.	2.3E+4	2.3E+4		1.5E+5	1.5E+5
	Ulcer	668.07	660.41		1.8E+4	1.9E+4
Entropy of Differences Histogram	Cancer	3.66	31.92	Nuclei Cytoplasm Ratio	0.73	0.87
	Gastritis	1.05	1.05		0.16	0.15
	I dyspl.	1.36	341.50		0.11	1.30
	T dyspl.	0.90	0.90		0.34	0.45
	Ulcer	8.7E+4	8.9E+3		0.79	0.78

Table 9 (continued)
Statistics of the data set

Nuclei per Cell	Cancer	1.00	0.96	Mean Distance of Nuclei in Cell	0.28	0.32
	Gastritis	0.22	0.22		0.42	0.42
	I dyspl.	0.33	0.18		0.24	0.43
	T dyspl.	0.25	0.25		-0.33	-0.44
	Ulcer	0.19	0.15		0.24	0.22
Mean Radius of Nuclei in Cell	Cancer	6.57	6.18			
	Gastritis	1.03	1.02			
	I dyspl.	1.54	0.68			
	T dyspl.	2.47	1.95			
	Ulcer	1.36	1.24			